Infection and Drug Resistance

Dovepress
open access to scientific and medical research

Open Access Full Text Article

ORIGINAL RESEARCH

Virus-Like Particles Assembled Using Respiratory Syncytial Virus Matrix Protein Elicit Protective Immunity in Mice

Su-Hwa Lee[1,*], Ki-Back Chu[2,*], Min-Ju Kim[3], Fu-Shi Quan[1,2]

[1]Department of Medical Zoology, School of Medicine, Kyung Hee University, Seoul, Republic of Korea; [2]Medical Research Center for Bioreaction to Reactive Oxygen Species and Biomedical Science Institute, Core Research Institute, School of Medicine, Kyung Hee University, Seoul, Republic of Korea; [3]Department of Biomedical Science, Graduate School, Kyung Hee University, Seoul, Republic of Korea

*These authors contributed equally to this work

Correspondence: Fu-Shi Quan, Department of Medical Zoology, School of Medicine, Kyung Hee University, 26, Kyungheedae-ro, Dongdaemun-gu, Seoul, 02447, Republic of Korea, Tel/Fax +82-2-961-2302, Email fsquan@khu.ac.kr

Purpose: Heterologous virus-like particle (VLP) assembly involving influenza or the Newcastle disease virus matrix protein (M) has been extensively used to explore the efficacies of VLP vaccines against the respiratory syncytial virus (RSV). Here, we attempted to generate homologous RSV VLPs by expressing the pre-fusion (pre-F) or the glycoprotein (G) on the RSV M protein and evaluated their protective efficacy in mice.

Methods: We generated VLPs using the baculovirus expression system in *Spodoptera frugiperda* (Sf9) insect cells. Recombinant baculoviruses expressing the RSV pre-F, G, and M antigens were inoculated into Sf9 cells, and particles were self-assembled. Mice were immunized with either pre-F or G-expressing VLPs, and immune parameters were assessed to determine protection.

Results: Our findings show that successful VLP assembly can be achieved by utilizing recombinant baculoviruses expressing the RSV pre-F or G proteins with the native matrix protein. Mice immunized with either pre-F or the G antigen-expressing VLPs elicited robust serum-mediated virus neutralization. VLP immunization evoked Th1-biased RSV-specific antibody responses in the sera of mice. Following challenge infection with the RSV A2 strain, immunized mice experienced lesser eosinophil and IL-4 accumulation in the lungs, though a substantial increase in TNF-α secretion was observed from CD4+ T cells. Interestingly, splenic antibody-secreting cell responses were substantially enhanced against RSV F antigen, but not against the RSV G antigen following immunization and challenge infection. Immunizing mice with the VLPs significantly inhibited pulmonary histopathology development, as indicated by the diminished inflammatory immune cell influx and mucin secretion.

Conclusion: Combined, these vaccine-induced immune responses contributed to successfully inhibiting the RSV replication in the lungs of mice and demonstrated that RSV VLP assembly using insect cell-derived homologous RSV matrix protein is a feasible approach.

Keywords: vaccine, protection, native virus antigen, recombinant baculovirus

Introduction

Virus-like particles (VLPs), since their emergence into the scientific limelight, have become a highly sought platform for vaccine development. Because VLPs do not possess any genetic materials necessary for progeny virus production, these nanoparticles are incapable of replicating in host cells or causing infection.[1] Numerous studies have identified various intrinsic properties contributing to their high immunogenicity such as their small size, surface charges promoting receptor interaction, and others.[2–4] Thus far, several VLP vaccines have been approved for commercial use by the United States Food and Drug Administration.[1] Driven by their success, VLP-based vaccine development for pathogens currently lacking efficacious prophylaxis tools such as the respiratory syncytial virus (RSV) has been ongoing. Though largely asymptomatic in healthy individuals, RSV infection is a major health hazard that can jeopardize the lives of infants, the

Received: 13 July 2023
Accepted: 1 September 2023
Published: 11 September 2023

elderly, and the immunocompromised.[5–7] Although two VLP vaccines manufactured by Virometix AG and Icosavax, Inc are in Phase 1 clinical trials, not a single efficacious RSV vaccine has been approved for clinical use to this day.

Research involving RSV VLP vaccines has only begun fairly recently. Initially, VLP assembly using entirely authentic RSV protein components was disregarded due to inefficient virion particle assembly resulting in low yields.[8] This led to the formation of heterologous VLPs using the protein components derived from the Newcastle disease virus, influenza virus, and others,[9–11] as the process of RSV VLP assembly was poorly understood at the time. Later studies did reveal that the RSV F, M, N, and P proteins are the minimum requirements for proper particle assembly, with phenylalanine residue in the F protein cytoplasmic tail and the M protein being integral for virion assembly.[12] Another study further attempted to understand authentic RSV VLP assembly and revealed that the P, M, and F carboxy terminus were sufficient for authentic RSV particle formation resembling that of native virions.[13] Similar to the F protein, the cytoplasmic tail portion of the RSV G was crucial for its co-localization with the RSV M protein as mutants lacking the cytoplasmic domain failed to coalesce into virions.[14] Recently, one study delineated the role of P and M interaction, which acts as a key regulator of RSV VLP budding.[15] Despite the advances in our understanding of VLP assembly, studies investigating the efficacy of native RSV VLP vaccines are severely lacking.

To date, only 2 studies assessed the vaccine potential of structurally authentic RSV VLPs in animal models. Mammalian cell-derived RSV VLPs expressing the F, G, and M proteins were demonstrated to be properly assembled and ensured that both lower and upper respiratory tracts of the immunized animals were protected again RSV challenge infection.[16] In another study, Vero cells were transfected with adenoviruses expressing the RSV F and M proteins for VLP assembly. A single immunization with these VLPs also elicited robust mucosal immunity and protected BALB/c mice.[17] Based on these findings, we reasoned that VLP assembly using native RSV antigen components using different protein expression systems could be an alternative option to mammalian cells which are relatively more expensive with limited scalability. To test the feasibility of this approach, we used insect cells for RSV VLP assembly and evaluated their immunogenicity. Our findings revealed that in line with the previous studies, VLPs eliciting protection can be assembled using native RSV M proteins in insect cells.

Materials and Methods

Animals and Ethics

Six-week-old female BALB/c mice were purchased from NARA Biotech (Seoul, Republic of Korea). All experimental procedures involving animals were approved by the Kyung Hee University IACUC (permit ID: KHSASP-21-340), which complies with the guidelines established by the Association for Assessment and Accreditation of Laboratory Animal Care (AAALAC). Immunization and blood collection were performed under mild anesthesia using isoflurane. Animals were housed in an institution-approved facility with 12 h day and night cycles, easy access to food and water, with environmental enrichments. Mice experiencing vision impairment following retro-orbital plexus puncture or weight loss exceeding 20% of the initial value were humanely euthanized in a CO_2 chamber. All efforts were made to minimize the number of animals used in the experiment as well as their suffering.

Cell Culture and Virus Preparation

For virus titration and neutralization assays, HEp-2 cells purchased from the ATCC (Manassas, VA, USA) were cultured in DMEM supplemented with 10% fetal bovine serum and 1% penicillin/streptomycin. Cells were maintained in an incubator with 5% CO_2 at 37°C. Viruses were also propagated using the HEp-2 cells. RSV A2 stocks were used to infect confluent monolayers of cells using serum-free media and cytopathological effects were monitored daily. Once the majority of the cells were infected, cells were gently detached from the plates using a cell scraper. After centrifuging the cells at 3000 RPM for 15 min, 4°C, pellets were resuspended in serum-free DMEM and sonicated. Following this procedure, contents were centrifuged at 2000 RPM, 4°C, 10 min, and the supernatant fraction containing the viruses were collected. Supernatants were aliquoted, titrated by immunostaining-based plaque assay,[18] and stored at −80°C until use.

RSV M Gene Cloning and VLP Assembly in Insect Cells

RSV M gene (GenBank: AAC14898.1) was cloned and expressed using the baculovirus expression system following the manufacturer's instructions (Thermo Fisher Scientific, Waltham, MA, USA). Polymerase chain reaction (PCR) primers for the

RSV M gene (F: 5'-AAAGGATCCACCATGGAAACATACGTGAACAAG-3'; R: 5'-TTACTCGAGTTAATCTTCCA TGGGTTTGAT-3') were purchased from Sigma-Aldrich (St. Louis, MO, USA). Briefly, genes were cloned into the pBlueScript vector and subcloned into the pFastBac vector. Gene insertion was confirmed by treating the transformant DNA with the restriction enzymes XbaI and XhoI (New England Biolabs, Ipswich, MA, USA). Successful clones were further transformed with DH10Bac competent cells and colony PCR was performed. Baculovirus-derived VLPs were constructed similar to the methods described in our previous study,[19] with the only change being the substitution of influenza M1 recombinant baculovirus (rBV) with RSV M rBV. In brief, *Spodoptera frugiperda* (Sf9) cells co-infected with the rBVs expressing RSV M with either RSV pre-F or the G antigen were cultured at 27°C in a shaking incubator. At 3 days post-infection (dpi), cell culture suspensions were centrifuged at 6000 RPM for 30 min and supernatants were collected. Ultracentrifuging the supernatants at 30,000 RPM for 1 h, 4°C resulted in sedimentation of the VLPs. After resuspending the VLPs in 1 mL of phosphate-buffered saline (PBS), the VLPs were overlaid on top of the sucrose density gradient for purification. Once the VLPs have been purified through sucrose density gradient, they were washed with PBS and protein concentrations were determined using Micro BCA Protein Assay Kit (ThermoFisher, Waltham, MA, USA).

Characterization of the VLPs

VLPs were characterized via transmission electron microscopy and Western blot following the methods previously described.[11] Briefly, VLPs stained with 2% uranyl acetate were observed using the Bio-High voltage EM system (JEM-1400 Plus at 120kV and JEM-1000BEF at 1000kV, JEOL Ltd., Tokyo, Japan) and checked for proper assembly. For Western blot analysis, VLPs were separated using 10% sodium dodecyl sulfate polyacrylamide gels. Proteins were transferred to a polyvinylidene difluoride membrane (Millipore, Burlington, MA, USA), blocked with 5% skim milk solution prepared in Tris-buffered saline with 0.1% Tween-20 (TBST) for 1 h at RT, and incubated overnight at 4°C with respective antibodies. For pre-F antigen, membranes were probed with anti-RSV F monoclonal antibody (1:5000 dilution in TBST; Abcam, Cambridge, UK). RSV-infected mouse sera and anti-RSV M mouse antibody (AbClon, Seoul, Republic of Korea) were used to detect RSV G and M antigens, respectively. After primary antibody incubation, membranes were probed with HRP-conjugated anti-mouse IgG and bands were developed using enhanced chemiluminescence. Images were acquired using ChemiDoc (Bio-Rad, Hercules, CA, USA).

VLP Immunization, RSV Challenge Infection, Serum Collection

Mice were randomly selected and separated into 6 different groups (n = 6 per group). Naïve mice were unimmunized and uninfected, whereas the naïve challenge group served as RSV infection controls. Mice in the pre-F+M and G+M groups were immunized twice with 100 μg of VLPs at 4-week intervals. For formalin-inactivated RSV (FI-RSV) and live RSV, mice were immunized once with either 50 μg of FI-RSV or 1×10^5 pfu of RSV A2, respectively. Four weeks after the final immunization, mice were challenged with 4×10^6 pfu of RSV A2 strain through the intranasal route. Blood samples were drawn from individual mice 4 weeks after each immunization through retro-orbital plexus puncture.

Serum-Mediated Virus Neutralization and Lung Virus Titer Quantification

Sera collected after the final immunization were used to evaluate serum-mediated virus neutralization. Acquired sera were inactivated at 56°C for 30 min and serially diluted using serum-free DMEM. Then, equal volumes of RSV A2 were mixed with the inactivated sera and incubated for 1 h at 37°C. Confluent monolayers of HEp-2 cells were infected with the serially diluted virus-serum mixtures for 1 h, 37°C, with 5% CO_2. After allowing the viruses to adsorb to cells, inoculum from the wells were aspirated and gently overlaid with 1% noble agar. Once the agar has solidified, plates were incubated for 3 days in the incubator at 37°C, 5% CO_2. Agar layers were carefully removed by gentle running streams of water and fixed with formalin-methanol fixative solution. Wells were sequentially incubated with anti-RSV F monoclonal antibody and anti-mouse IgG-HRP secondary antibodies. Chromogenic substrate diaminobenzidine was used to visualize virus plaque formations, which were manually counted for virus quantification. Plaque assays were conducted following the method described above, with the only change being the use of serially diluted lung homogenates in place of serum-virus mixtures.

RSV-Specific Antibody Response Assessment

Sera were collected at regular intervals after prime and boost immunizations. Virus-specific antibodies were detected from the sera by enzyme-linked immunosorbent assay (ELISA) following the method previously described. Immunoplates were coated with either RSV F or G proteins (Sino Biological, Beijing, China) at 1 μg/mL in carbonate coating buffer overnight at 4°C. After blocking the wells with 0.2% gelatin prepared in PBS with 0.1% Tween-20 (PBST) at 37°C, 1 h, diluted immune sera (1:100 in PBS) were added to respective wells. Plates were incubated for 1 h at 37°C, washed three times with PBST, and incubated with horseradish peroxidase (HRP)-conjugated IgG subclasses (1:1000 dilution in PBS) at 37°C for 1 h. After the final washing step, o-phenylenediamine (OPD) substrate was dissolved in citrate substrate buffer and added to each well. Color development was measured by reading the absorbance values at 450 nm using a microplate reader (Enzo Life Sciences, Inc., Farmingdale, NY, USA).

Flow Cytometry Analysis of Immune Cell Populations

Lung cells were separated using Percoll density gradient solution for flow cytometry analysis as described previously.[20] Fluorophore-conjugated CD11b, CD125, and Siglec-F antibodies were used to detect eosinophils. For intracellular cytokine production, lung cells stained with CD3 and CD4 antibodies were permeabilized following the manufacturer's instructions (BD Cytofix/Cytoperm; BD Biosciences, Franklin Lakes, NJ, USA) and subsequently stained with TNF-α, and IL-4 antibodies. All fluorophore-conjugated antibodies were purchased from BD Biosciences (Franklin Lakes, NJ, USA).

Splenic Antibody-Secreting Cell (ASC) Response Detection

Single cell populations of murine splenocytes were prepared by homogenizing the spleen tissues with autoclaved slide glasses with RPMI-1640 media. Cell strainers were used to remove tissue debris and contents were centrifuged. After removing the supernatants, red blood cells (RBCs) were lysed with RBC lysis buffer following the manufacturer's instructions (Sigma-Aldrich, St. Louis, MO, USA). After RBC removal, splenocytes were resuspended in fresh RPMI-1640 media and counted with a hemacytometer. In 96-well immunoplates coated with RSV F or G proteins, splenocytes acquired from each group were seeded and incubated at 37°C for 5 days. Supernatants were removed from the wells and anti-mouse IgG or IgA antibodies were added to respective wells. After incubating the plate for 1 h at 37°C, wells were washed with PBST and OPD substrate solutions were inoculated into wells for color development. Optical density readings at 450 nm were measured using a microplate reader.

Histopathological Assessment of Pulmonary Inflammation

A small piece of lung cross-section was acquired from each mouse by cutting horizontally along the inferior lobes. Lung tissues were stored in 10% formalin solution prior to histopathological examination. Paraffin-embedded tissue cross-sections were stained using hematoxylin and eosin (H&E) or periodic acid-Schiff (PAS). Pathological changes were examined under the microscope and blindly scored based on their severity on a scale of 0 to 5 as previously described.[21]

Statistical Analysis

All samples were individually processed and data sets were presented as mean ± SD. Statistical significance between groups was determined via one-way analysis of variance with Tukey's post hoc tests. All statistical tests were performed using the Prism 8 software (GraphPad, CA, USA). Asterisks were used to indicate statistical significance (*$p < 0.05$, **$p < 0.01$, ***$p < 0.001$).

Results

Virus-Like Particle Generation and Their Characterization

RSV M gene, the core protein of the VLPs used in the present study was PCR-amplified, initially cloned into the pBlueScript and then subcloned into the pFastBac vector (Figure 1A). Baculovirus expressing RSV M was generated and these were co-transfected into Sf9 cells along with RSV pre-F and G rBVs for VLP assembly. As expected, VLPs with

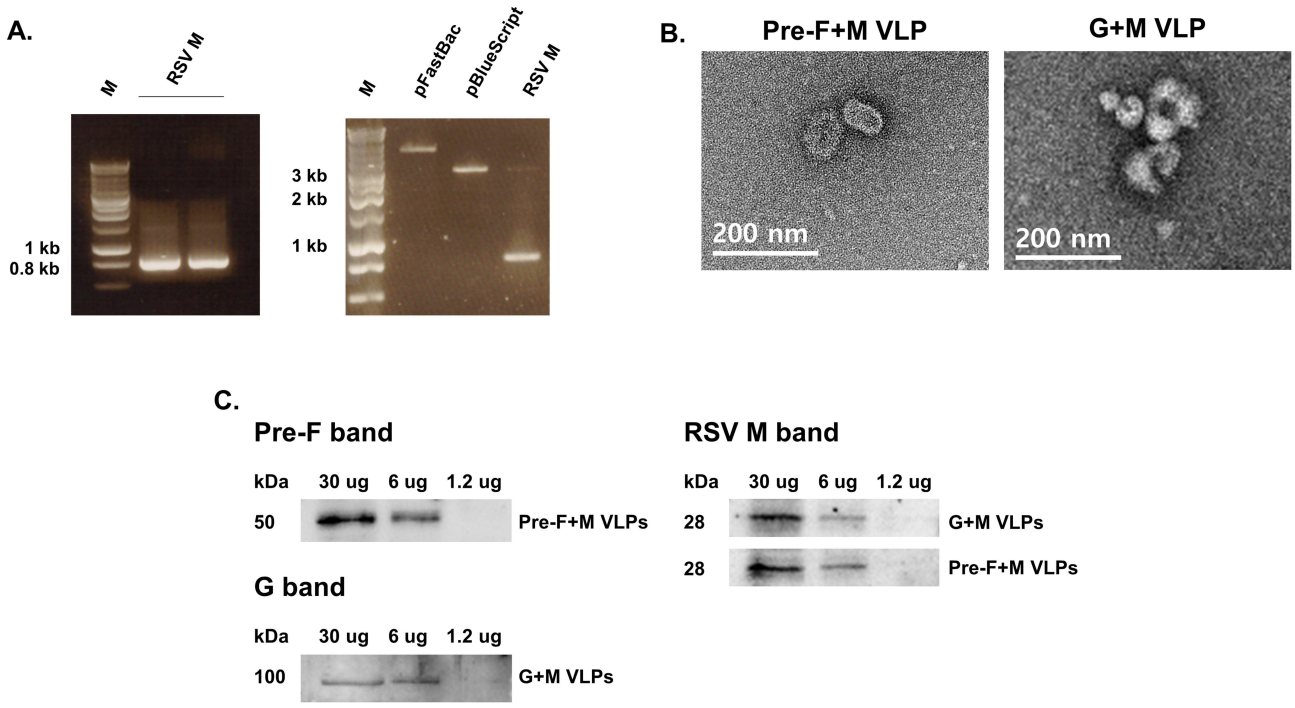

Figure 1 Characterization of RSV VLP constructs generated using native RSV antigens. The gene corresponding to the RSV matrix protein was PCR-amplified (**A**, left panel). Successful integration of the RSV M gene into the pFastBac vector was confirmed through restriction enzyme digestion (**A**, right panel). Morphological features of the VLPs were examined under the transmission electron microscope (**B**). Western blots were performed to confirm successful expression of native RSV components (**C**).

sizes ranging from 100 nm to 200 nm were visualized under the TEM (Figure 1B). To confirm successful self-assembly of the RSV VLPs, Western blots were performed (Figure 1C). Respective bands corresponding to the RSV pre-F, G, and M proteins were confirmed.

Immunization Induces Antibody Responses in the Sera of Mice

To confirm the presence of RSV-specific antibodies in the sera of mice, blood samples were drawn at regular intervals and ELISA was performed. As expected, immunization did elicit virus-specific serum antibody responses. Against RSV F antigen, IgG antibody responses were predominantly elicited by pre-F+M VLP and live RSV immunization group (Figure 2A). Although FI-RSV immunization did increase IgG responses against the RSV F antigen, they were raised to negligible levels. Identical findings were observed from IgG2a and 2b as significantly enhanced antibody responses were solely detected from pre-F+M and live RSV groups. Yet, none of the immunization groups were capable of eliciting RSV-specific IgG1 responses. Interesting findings were observed when ELISA was performed against RSV G antigen (Figure 2B). Here, only G+M VLP and live RSV immunization managed to elicit significantly increased IgG responses, whereas marginal increases were observed from pre-F+M and FI-RSV groups. As with RSV F antigen ELISA, hardly any IgG1 responses were elicited against the RSV G protein. IgG2a responses against RSV G antigen were restricted to G+M VLP and live RSV groups, but even these groups failed to evoke noticeable levels of IgG2b serum antibody responses. Sera were collected from VLP-immunized mice to assess RSV-neutralizing activity (Figure 2C). As expected, serum-mediated neutralizing activity was not detected from PBS control. Background levels of neutralizing activity were observed until 300-fold dilution for naïve sera, which rapidly waned with subsequent dilutions. VLP immune sera retained their neutralizing potential even until 2700-fold dilution.

VLP Immunization Elicits ASC Responses in the Spleens of Mice

Splenocytes were stimulated with RSV F or G antigens for ASC response assessment. In splenocytes stimulated with the RSV F antigens, profound IgG and IgA levels were detected only from the pre-F+M VLP and live RSV groups. Marginal increases in IgG and IgA levels were elicited by G+M VLP immunization, but changes were negligible compared to

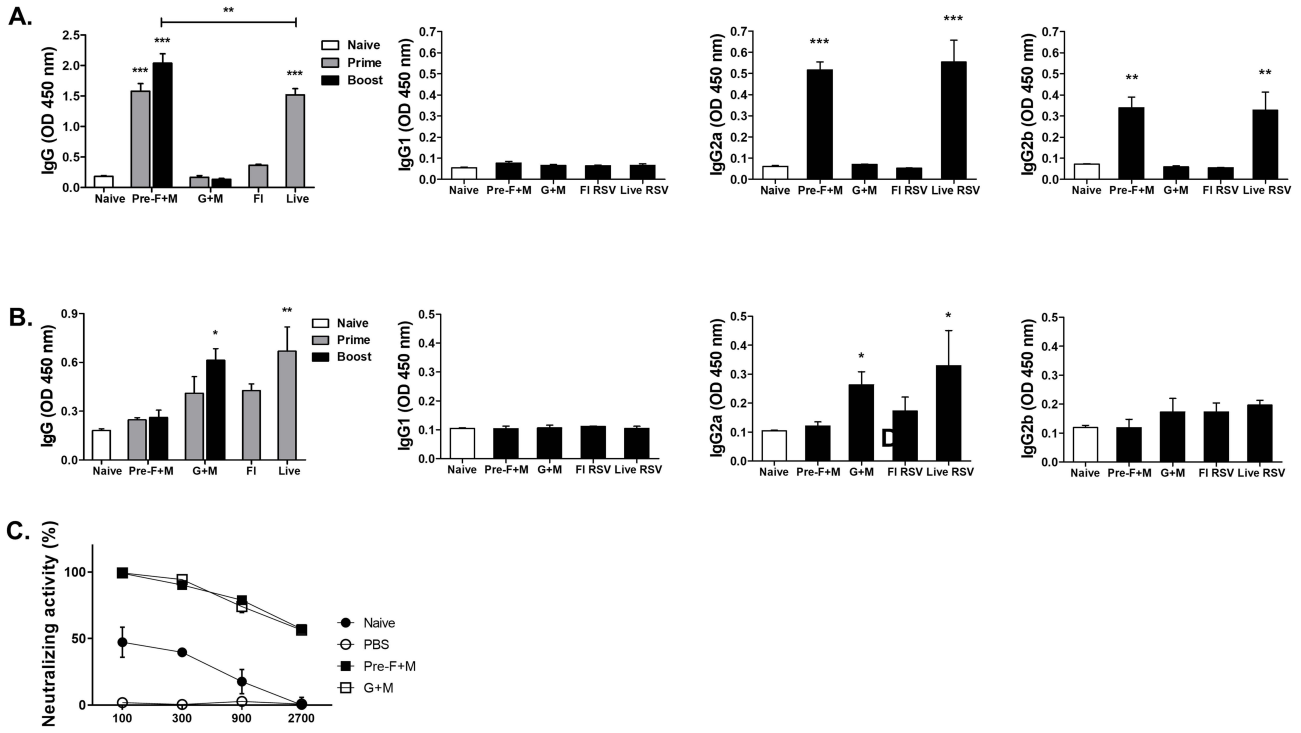

Figure 2 Serum antibody response. ELISA was performed to confirm successful induction of RSV-specific antibody responses. Virus-specific IgG, IgG1, IgG2a, and IgG2b responses were assessed against RSV F (**A**) and RSV G (**B**) antigens. Sera acquired from the VLP immunization groups after the second immunization were used to evaluate serum-mediated virus neutralization. Plaque reductions compared to the controls at various dilutions were used to determine the RSV neutralizing activity (**C**). Asterisks denote statistical significance compared to the naïve control, and p values less than 0.05 were considered statistically significant (*p < 0.05, **p < 0.01, ***p < 0.001). Data are presented as mean ± SD.

naïve challenge control. FI-RSV immunization induced a significant increase in IgG but not IgA (Figure 3A). Contrary to this finding, they were different for the splenocytes stimulated using RSV G protein. Significant increases in IgG and IgA were only elicited by live RSV immunization and none of the VLPs were capable of eliciting substantial ASC responses (Figure 3B).

Lung Virus Titer Quantification in Vaccinated Mice

Lung virus titers were quantified via plaque assay. Representative microscopic images of RSV plaque formation, indicated by the circular brown precipitates, were provided for each group (Figure 4A). As expected, plaques were not detected from naïve mice. While a large number of plaques were detected in the naive challenge group, significantly fewer plaques were observed from the lung supernatants of VLP-immunized mice. Live RSV immunization exhibited the lowest plaque formation, whereas the highest plaque counts were visualized from the FI-RSV group. Quantified lung virus titers were consistent with the visual findings (Figure 4B). Plaques were undetected in naïve and live RSV groups, while virus titers exceeding 1500 pfu/mL were detected from naïve challenge and FI-RSV groups. VLP immunization, regardless of pre-F or G protein expression, significantly reduced the lung virus titers when compared to the naïve challenge group.

Histopathological Evaluation of Pulmonary Inflammation Post-Challenge Infection

To confirm the extent of pulmonary inflammation inhibited by vaccines, murine lung tissues were subjected to histopathological examinations. Representative images for each group were acquired via H&E and PAS staining. Scores were provided after randomly assessing images under the microscope based on their pathogenic severity. Briefly, not much cellular influx was observed for naïve control. Upon RSV infection, a massive influx of cells was noted and the same applied to the FI-RSV group. On the contrary, mice receiving either pre-F+M or G+M VLPs were protected and severe pathogenicity was not detected. This was also the case for the live RSV immunization group (Figure 5A and B). Patterns were slightly different for the PAS staining when compared to the H&E. Consistent with our

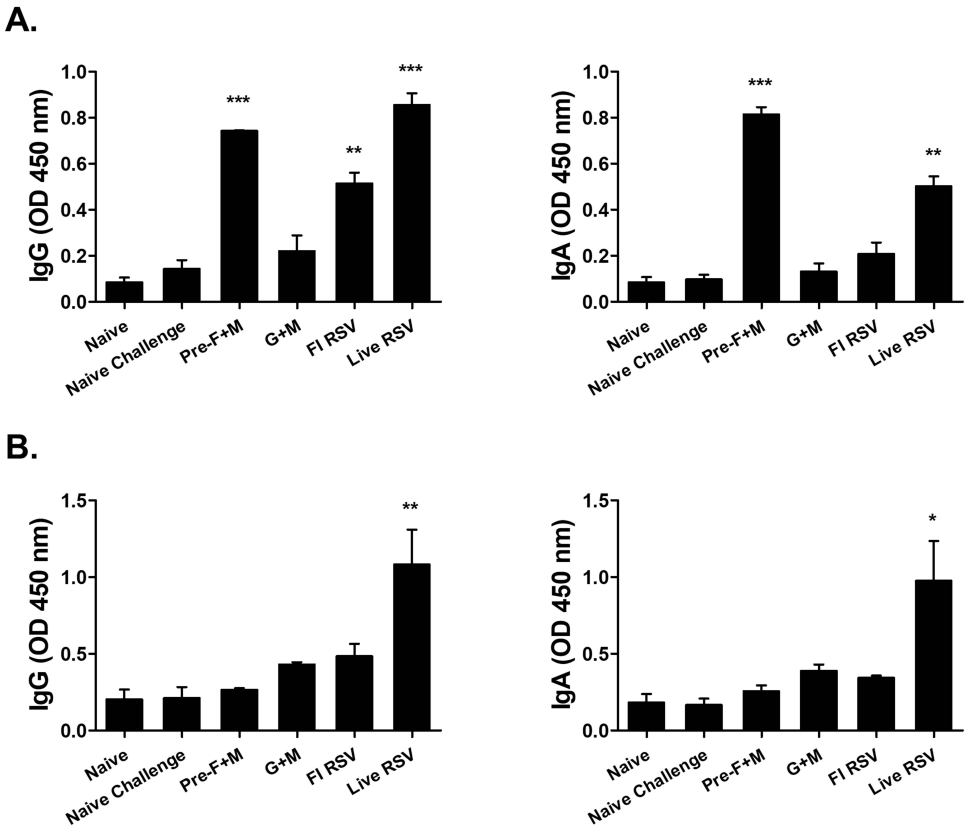

Figure 3 Splenic antibody-secreting cell response detection. Isolated single cell populations of splenocytes were cultured with either RSV F (**A**) or RSV G (**B**) antigens. After culturing the splenocytes for 5 days, supernatants were removed and HRP-conjugated IgG subclass antibodies were inoculated into respective wells. Optical density readings were measured to assess ASC responses. Asterisks denote statistical significance compared to the naïve challenge control, and p values less than 0.05 were considered statistically significant (*p < 0.05, **p < 0.01, ***p < 0.001). Data are presented as mean ± SD.

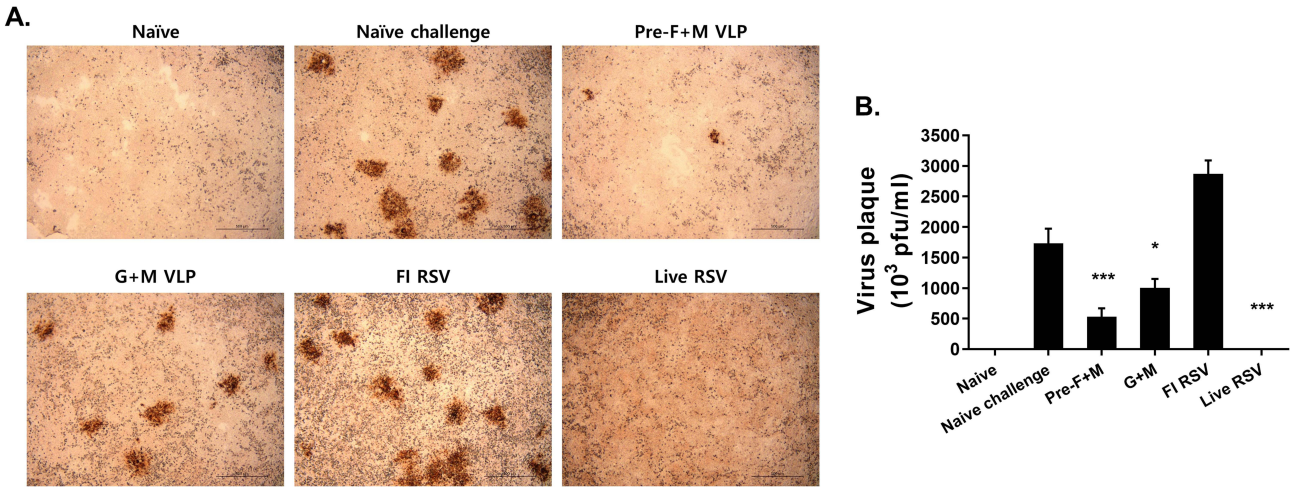

Figure 4 Lung virus titer reduction. Plaque assays were performed using the immunostaining method. Plaques, surrounded by brown precipitates following DAB staining, were visualized under the microscope (**A**). Plaques were enumerated and final virus titers were calculated for all groups (**B**). Asterisks denote statistical significance compared to the naïve challenge control, and p values less than 0.05 were considered statistically significant (*p < 0.05, ***p < 0.001). Data are presented as mean ± SD.

previous findings, mucin production was predominantly detected from the FI-RSV group, while they were only detected to a small extent in the other immunization groups. Magenta-colored mucin secretions were denoted using arrows (Figure 5C). PAS scores from randomly selected fields of views were determined and plotted. Compared to the FI-RSV immunization group, substantially lower scores were detected from the other 3 immunization groups (Figure 5D).

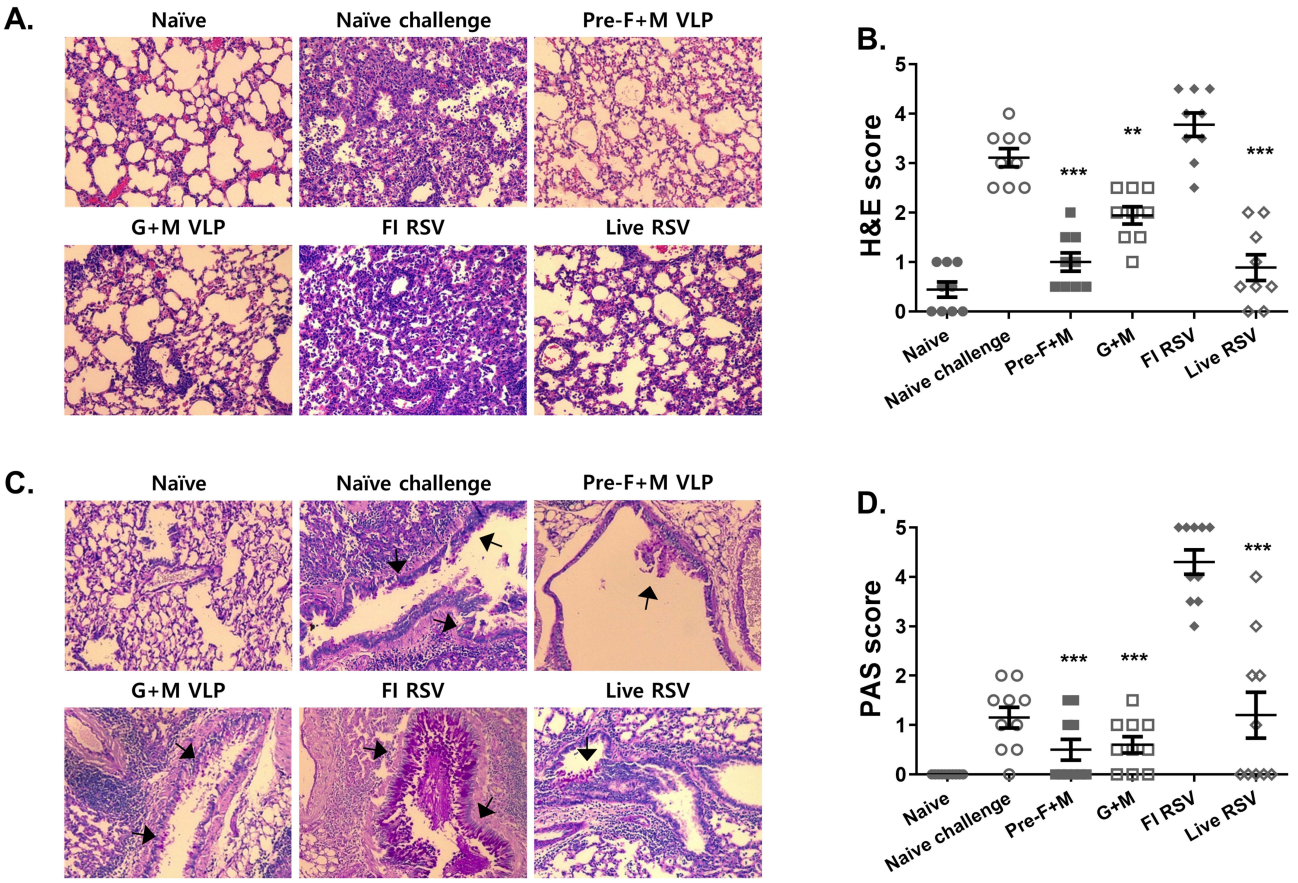

Figure 5 Lung histopathology evaluation. Lung tissue cross-sections were stained to assess the severity of pulmonary inflammation. Representative images from H&E stains were provided for each group (**A**). Randomly selected fields of view were scored based on the scoring criteria (**B**). PAS-stained images depicting mucin production were shown (**C**). Magenta-colored mucin secretions were indicated using arrows. Lung sections were scored based on their severity (**D**). Asterisks denote statistical significance compared to the naïve challenge control, and p values less than 0.05 were considered statistically significant (**p < 0.01, ***p < 0.001). Data are presented as mean ± SD. Symbols in each group indicate individual histopathology scores for the corresponding group mentioned in the x-axis. All images were acquired under 200x magnification.

Flow Cytometric Assessment of Pulmonary Immune Cell Influx Following Immunization

Flow cytometry was performed to evaluate the proliferation of immune cell populations in the lung tissues. Lung cell suspensions were gated as displayed in the gating strategy to evaluate eosinophils and intracellular cytokine-secreting CD4+ T cells (Figure 6A). As expected, enhanced pulmonary eosinophilia was detected from both naïve challenge and FI-RSV groups (Figure 6B). Compared to the FI-RSV group, significant reductions were observed in mice immunized with live RSV or VLP vaccines. In VLP-immunized mice, eosinophil populations were detected to near basal levels, whereas eosinophil percentages for live RSV resembled that of the naïve challenge group. IL-4 and TNF-α secretions were evaluated in permeabilized lung CD4+ T cells via flow cytometry. Pre-F+M VLP immunization significantly reduced IL-4 secretion to basal levels in comparison to the naïve challenge. While particle reductions were observed from the other groups, they were not statistically significant (Figure 6C). TNF-α secretions were substantially enhanced following immunization. Specifically, they were only enhanced by VLPs and live RSV but not by FI-RSV immunization (Figure 6D).

Discussion

The present study aimed to confirm whether or not RSV VLP assembly using structurally native components is feasible in recombinant baculovirus-derived insect cell lines. Our findings illustrated that as was the case in mammalian cells, efficient assembly of quasi-authentic RSV VLPs can be also achieved in insect cell lines. Furthermore, native RSV-resembling VLP immunization in mice contributed to suppressing RSV replication and ultimately lessened the lung virus

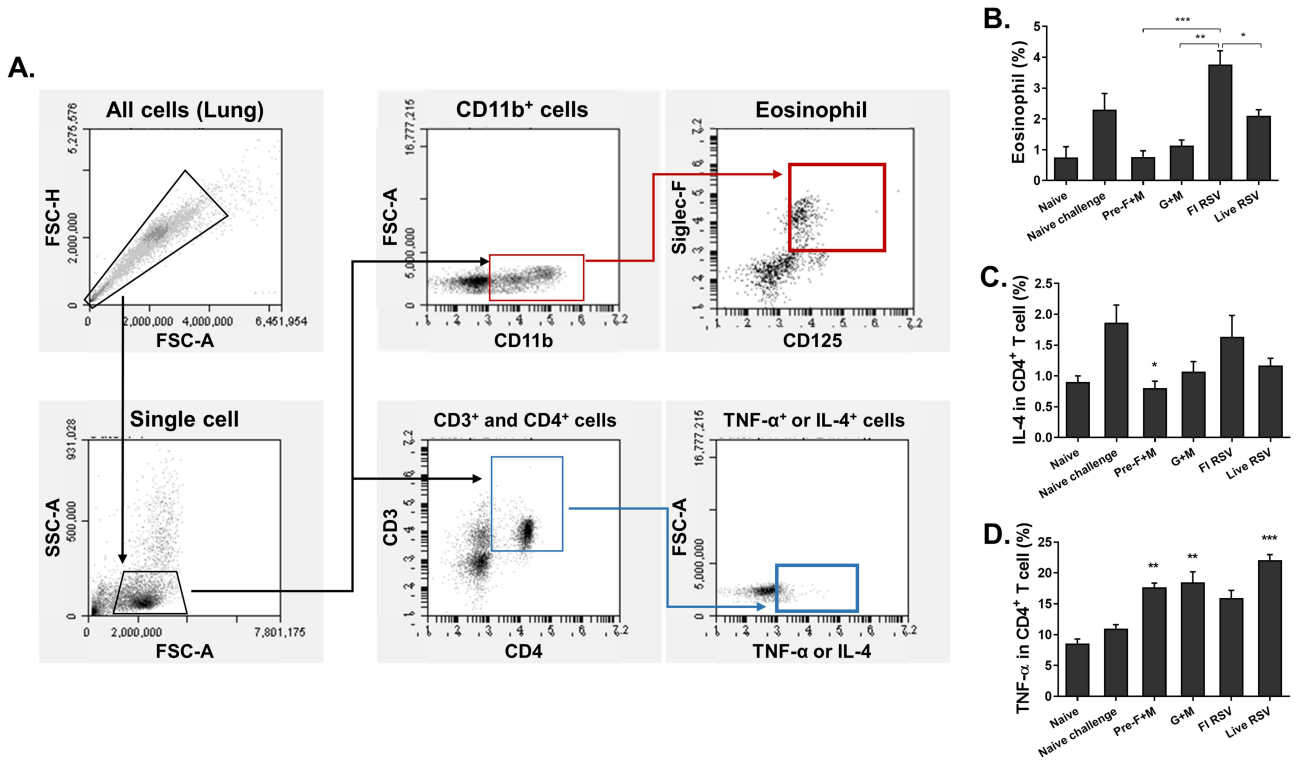

Figure 6 Flow cytometry assessment of murine lung cell populations. Lung cells were subjected to flow cytometry analysis. Single cell populations were prepared to evaluate eosinophils and intracellular cytokine inductions. Cells were gated based on their appropriate surface markers and stained following the strategy outlined above (**A**). Stained lung cell eosinophil populations (**B**), IL-4-secreting CD4+ T cells (**C**), and TNF-α-secreting CD4+ T cells (**D**) were assessed. Asterisks denote statistical significance compared to the naïve challenge control, and p values less than 0.05 were considered statistically significant (*p < 0.05, **p < 0.01, ***p < 0.001). Data are presented as mean ± SD.

titers in vivo. Based on the findings presented here, the feasibility of this approach should be further confirmed in other protein expression systems such as plants, yeast, or even bacteria.

The overall protective immunity elicited in mice was to be expected, as demonstrated through earlier studies published by other research groups in mammalian cells. Much of the findings observed here are consistent with the results acquired from mammalian cell-derived authentic RSV VLP immunization, despite the differences in immunization regimen.[17] Mammalian cell-derived VLP immunization elicited robust RSV F-specific serum IgG2a responses than IgG1 in mice. The degree of alveolitis, interstitial pneumonia, and peribronchiolar inflammation occurred to a lesser extent in the lungs of VLP-immunized mice, implying that insect cell-derived VLPs can evoke immune responses similar to those observed from VLPs of mammalian cell origin. IL-4 has important implications for the development of immune pathogenesis. RSV infection frequently disrupts the Th1/Th2 balance and leads to elevated levels of Th2 cytokine such as IL-4 in infants, which consequently leads to eosinophilia and airway hyperresponsiveness.[22,23] Consistent with this notion, in the present study, VLP immunization suppressed excessive IL-4 secretions by CD4+ T cells which were not observed from naïve challenge or the FI-RSV groups. These results are similar to the RSV VLP-mediated protection reported by other groups. Kim et al[24] reported a significantly lesser degree of IL-4 cytokine levels in the bronchoalveolar lavage fluids (BALF) of RSV VLP-immunized mice. This is also supported by high basal levels of IL-4-producing CD4+ T cells in RSV-infected neonates.[25]

TNF-α results observed in our study were partly similar to previous findings. TNF-α expressions were markedly increased in the BALF of RSV F VLP-immunized mice, even compared to that of the FI-RSV control group.[24] Pulmonary TNF-α secretion was also enhanced in VLP-immunization groups compared to the FI-RSV in this study. The exact role of TNF-α in RSV immunopathology remains largely unknown and conflicting findings have been reported. For example, studies have provided evidence for TNF-α inducing weight loss in mice while other studies reported no significant difference even after TNF-α ablation via antibody treatment.[26,27] Discrepancies were also reported in clinical studies. In one study, children experiencing substantially less TNF-α production via CD4+ T cells were prone to developing recurring wheezing.[28] In another clinical study, increased

CD4+ T cell TNF-α responses were associated with disease severity.[29] In our study, TNF-α secretion occurred to a greater extent which was comparable to those of FI-RSV or the naïve challenge controls. While the exact cause of this excessive TNF-α production in VLP-treated mice remains elusive, it is highly plausible that their expression only plays a minor role in pulmonary inflammation. Evidently, despite the TNF-α production, immune cell influx or mucin secretions were only marginally greater than that of naïve mice.

One of the major limitations of using insect cell-derived recombinant protein as vaccine antigen is the issue arising from post-translational modification (PTMs). In mammalian cell lines, RSV antigens are subjected to PTMs that highly resemble those that occur in humans. Contrary to this, N-linked glycosylations frequently observed in humans are lacking in insect cell-derived proteins. Fortunately, this issue could be resolved thanks to advances in biotechnology. Several studies have identified methods that enable mammalian-like PTMs, especially glycosylation in insect cell lines. An Sf9 cell line with integrated mammalian glycosyltransferases was capable of eliciting complex N-linked glycosylation found in mammals.[30] Other genetic engineering techniques can also be used to promote human-type glycosylation in insect cells.[31,32] Assessing the extent of this effect on insect cell line expression is beyond the scope of this study, but it is plausible that RSV proteins expressed under these conditions would resemble those that are expressed in human or mammalian cell lines. Further studies confirming this would be beneficial for the rational design of RSV vaccines.

Conclusion

In conclusion, we have demonstrated that quasi-authentic RSV VLPs can be properly assembled using the baculovirus expression system. When RSV pre-F or G VLPs generated this way were administered into mice, immune responses were elicited to counteract the pulmonary pathologies inflicted by RSV A2 challenge infection. Further studies comparing the efficacies of chimeric RSV VLPs to those of authentic RSV VLPs should be carefully conducted to identify factors accounting for discrepancies in protection, if any.

Abbreviations

ASC, antibody-secreting cell; dpi, days post-infection; FI-RSV, formalin-inactivated RSV; PBS, phosphate-buffered saline; rBV, recombinant baculovirus; RSV, respiratory syncytial virus; VLP, virus-like particle.

Ethics Approval

All experimental procedures and animal handling were approved by Kyung Hee University's Institutional Animal Care and Use Committee (IACUC, permit ID: KHSASP-21-340) and performed following the Animals in Research: Reporting In Vivo Experiments (ARRIVE) guidelines.

Funding

This study was financially supported by the Core Research Institute (CRI) Program, the Basic Science Research Program through the National Research Foundation of Korea (NRF), Ministry of Education (NRF-2018-R1A6A1A03025124) and the Ministry of Health & Welfare, Korea (HV20C0142).

Disclosure

The authors report no conflicts of interest in this work.

References

1. Kushnir N, Streatfield SJ, Yusibov V. Virus-like particles as a highly efficient vaccine platform: diversity of targets and production systems and advances in clinical development. *Vaccine*. 2012;31(1):58–83. doi:10.1016/j.vaccine.2012.10.083
2. Mohsen MO, Gomes AC, Cabral-Miranda G, et al. Delivering adjuvants and antigens in separate nanoparticles eliminates the need of physical linkage for effective vaccination. *J Control Release*. 2017;251:92–100. doi:10.1016/j.jconrel.2017.02.031
3. Bachmann MF, Jennings GT. Vaccine delivery: a matter of size, geometry, kinetics and molecular patterns. *Nat Rev Immunol*. 2010;10(11):787–796. doi:10.1038/nri2868
4. Chu KB, Quan FS. Virus-like particle vaccines against respiratory viruses and protozoan parasites. *Curr Top Microbiol Immunol*. 2021. doi:10.1007/82_2021_232

5. Shi T, McAllister DA, O'Brien KL, et al. Global, regional, and national disease burden estimates of acute lower respiratory infections due to respiratory syncytial virus in young children in 2015: a systematic review and modelling study. *Lancet*. 2017;390(10098):946–958. doi:10.1016/s0140-6736(17)30938-8
6. Tseng HF, Sy LS, Ackerson B, et al. Severe morbidity and short- and mid- to long-term mortality in older adults hospitalized with respiratory syncytial virus infection. *J Infect Dis*. 2020;222(8):1298–1310. doi:10.1093/infdis/jiaa361
7. Pilie P, Werbel WA, Riddell J, Shu X, Schaubel D, Gregg KS. Adult patients with respiratory syncytial virus infection: impact of solid organ and hematopoietic stem cell transplantation on outcomes. *Transpl Infect Dis*. 2015;17(4):551–557. doi:10.1111/tid.12409
8. McGinnes LW, Gravel KA, Finberg RW, et al. Assembly and immunological properties of Newcastle disease virus-like particles containing the respiratory syncytial virus F and G proteins. *J Virol*. 2011;85(1):366–377. doi:10.1128/jvi.01861-10
9. Lee S, Quan FS, Kwon Y, et al. Additive protection induced by mixed virus-like particles presenting respiratory syncytial virus fusion or attachment glycoproteins. *Antiviral Res*. 2014;111:129–135. doi:10.1016/j.antiviral.2014.09.005
10. Murawski MR, McGinnes LW, Finberg RW, et al. Newcastle disease virus-like particles containing respiratory syncytial virus G protein induced protection in BALB/c mice, with no evidence of immunopathology. *J Virol*. 2010;84(2):1110–1123. doi:10.1128/jvi.01709-09
11. Lee S-H, Chu K-B, Kim M-J, et al. Virus-like particle vaccine expressing the respiratory syncytial virus pre-fusion and G proteins confers protection against RSV challenge infection. *Pharmaceutics*. 2023;15(3):782. doi:10.3390/pharmaceutics15030782
12. Shaikh FY, Cox RG, Lifland AW, et al. A critical phenylalanine residue in the respiratory syncytial virus fusion protein cytoplasmic tail mediates assembly of internal viral proteins into viral filaments and particles. *mBio*. 2012;3(1). doi:10.1128/mBio.00270-11
13. Meshram CD, Baviskar PS, Ognibene CM, Oomens AGP, García-Sastre A. The respiratory syncytial virus phosphoprotein, matrix protein, and fusion protein carboxy-terminal domain drive efficient filamentous virus-like particle formation. *J Virol*. 2016;90(23):10612–10628. doi:10.1128/jvi.01193-16
14. Ghildyal R, Li D, Peroulis I, et al. Interaction between the respiratory syncytial virus G glycoprotein cytoplasmic domain and the matrix protein. *J Gen Virol*. 2005;86(Pt 7):1879–1884. doi:10.1099/vir.0.80829-0
15. Bajorek M, Galloux M, Richard CA, et al. Tetramerization of phosphoprotein is essential for respiratory syncytial virus budding while its N terminal region mediates direct interactions with the matrix protein. *J Virol*. 2021;95(7). doi:10.1128/jvi.02217-20
16. Walpita P, Johns LM, Tandon R, Moore ML. Mammalian cell-derived respiratory syncytial virus-like particles protect the lower as well as the upper respiratory tract. *PLoS One*. 2015;10(7):e0130755. doi:10.1371/journal.pone.0130755
17. Jiao YY, Fu YH, Yan YF, et al. A single intranasal administration of virus-like particle vaccine induces an efficient protection for mice against human respiratory syncytial virus. *Antiviral Res*. 2017;144:57–69. doi:10.1016/j.antiviral.2017.05.005
18. Kim KS, Kim AR, Piao Y, Lee JH, Quan FS. A rapid, simple, and accurate plaque assay for human respiratory syncytial virus (HRSV). *J Immunol Methods*. 2017;446:15–20. doi:10.1016/j.jim.2017.03.020
19. Chu KB, Lee SH, Kim MJ, Kim AR, Moon EK, Quan FS. Virus-like particles coexpressing the PreF and Gt antigens of respiratory syncytial virus confer protection in mice. *Nanomedicine*. 2022;17(17):1159–1171. doi:10.2217/nnm-2022-0082
20. Kim KH, Li Z, Bhatnagar N, et al. Universal protection against influenza viruses by multi-subtype neuraminidase and M2 ectodomain virus-like particle. *PLoS Pathog*. 2022;18(8):e1010755. doi:10.1371/journal.ppat.1010755
21. Kim AR, Lee DH, Lee SH, Rubino I, Choi HJ, Quan FS. Protection induced by virus-like particle vaccine containing tandem repeat gene of respiratory syncytial virus G protein. *PLoS One*. 2018;13(1):e0191277. doi:10.1371/journal.pone.0191277
22. Sung RY, Hui SH, Wong CK, Lam CW, Yin J. A comparison of cytokine responses in respiratory syncytial virus and influenza A infections in infants. *Eur J Pediatr*. 2001;160(2):117–122. doi:10.1007/s004310000676
23. Bermejo-Martin JF, Garcia-Arevalo MC, De Lejarazu RO, et al. Predominance of Th2 cytokines, CXC chemokines and innate immunity mediators at the mucosal level during severe respiratory syncytial virus infection in children. *Eur Cytokine Netw*. 2007;18(3):162–167. doi:10.1684/ecn.2007.0096
24. Kim KH, Lee YT, Hwang HS, et al. Virus-like particle vaccine containing the F protein of respiratory syncytial virus confers protection without pulmonary disease by modulating specific subsets of dendritic cells and effector T cells. *J Virol*. 2015;89(22):11692–11705. doi:10.1128/jvi.02018-15
25. Démoulins T, Brügger M, Zumkehr B, et al. The specific features of the developing T cell compartment of the neonatal lung are a determinant of respiratory syncytial virus immunopathogenesis. *PLoS Pathog*. 2021;17(4):e1009529. doi:10.1371/journal.ppat.1009529
26. Rutigliano JA, Graham BS. Prolonged production of TNF-alpha exacerbates illness during respiratory syncytial virus infection. *J Immunol*. 2004;173(5):3408–3417. doi:10.4049/jimmunol.173.5.3408
27. Ostler T, Davidson W, Ehl S. Virus clearance and immunopathology by CD8(+) T cells during infection with respiratory syncytial virus are mediated by IFN-gamma. *Eur J Immunol*. 2002;32(8):2117–2123. doi:10.1002/1521-4141(200208)32:8
28. Kitcharoensakkul M, Bacharier LB, Yin-Declue H, et al. Impaired tumor necrosis factor-α secretion by CD4 T cells during respiratory syncytial virus bronchiolitis associated with recurrent wheeze. *Immun Inflamm Dis*. 2020;8(1):30–39. doi:10.1002/iid3.281
29. Roumanes D, Falsey AR, Quataert S, et al. T-cell responses in adults during natural respiratory syncytial virus infection. *J Infect Dis*. 2018;218(3):418–428. doi:10.1093/infdis/jiy016
30. Legardinier S, Klett D, Poirier JC, Combarnous Y, Cahoreau C. Mammalian-like nonsialyl complex-type N-glycosylation of equine gonadotropins in Mimic insect cells. *Glycobiology*. 2005;15(8):776–790. doi:10.1093/glycob/cwi060
31. Toth AM, Kuo CW, Khoo KH, Jarvis DL. A new insect cell glycoengineering approach provides baculovirus-inducible glycogene expression and increases human-type glycosylation efficiency. *J Biotechnol*. 2014;182–183:19–29. doi:10.1016/j.jbiotec.2014.04.011
32. Chavez-Pena C, Kamen AA. RNA interference technology to improve the baculovirus-insect cell expression system. *Biotechnol Adv*. 2018;36(2):443–451. doi:10.1016/j.biotechadv.2018.01.008